International Journal on
"Technical and Physical Problems of Engineering"
(IJTPE)
Published by International Organization of IOTPE

ISSN 2077-3528
IJTPE Journal
www.iotpe.com
ijtpe@iotpe.com

June 2014 | Issue 19 | Volume 6 | Number 2 | Pages 145-152

CONTROLLER DESIGN FOR A DC-MICROGRID PV CONVERTER BASED ON ASYMMETRICAL Γ-SOURCE INVERTER CONSIDERING THE SUN TRACKER OPERATION

F. Khoshkhati [1] S. Toofan [2] B. Asaei [1]

1. Department of Electrical and computer Engineering, University of Tehran, Tehran, Iran
f.khoshkhati@gmail.com, b.asaei@ut.ac.ir
2. Department of Electrical and computer Engineering, University of Zanjan, Zanjan, Iran, s.toofan@znu.ac.ir

Abstract- This paper presents a power electronic interface (PEI) converter with three ports to connect a Photovoltaic system and a DC-microgrid to the main grid. The proposed converter is based on asymmetric Γ-source inverter, which makes two controllable ports in its DC side without utilizing any excessive DC/DC converters, which make it interesting for multi-port applications. The PEI system is expected to regulate DC-microgrid voltage to its reference voltage while keeping PV voltage to its reference value provided by maximum power point tracking (MPPT) algorithm in a certain direction of the PV panel determined by sun tracker controller (STC). For avoiding interference between STC system and MPPT algorithm, the PV voltage controller is designed much faster than STC, therefore until the next updating of the PV panel direction, the PV voltage controller can change PV voltage in some steps to find maximum power point. To this aim, the dynamic model of the PEI system is obtained using average state model and the appropriate control system is designed based on dynamic model of the system. According to the two degree of freedom in asymmetric Γ-source inverter pulse width modulation composed of inverter modulation index and inverter shoot through duty cycle, the control system are able to control DC-microgrid and PV voltage independently. The inverter shoot through duty cycle is used to control the PV voltage while the inverter modulation index, which is generated in AC current controller, is utilized for regulating the DC-microgrid voltage. The performance of the proposed control system for creating a DC-microgrid PV system is evaluated using simulation in MATLAB/Simulink.

Keywords: Power Electronic Interface (PEI), Photovoltaic, DC-Microgrid, Asymmetrical Γ-Source Inverter.

I. INTRODUCTION

In recent years due to reduction in fossil cell resources and increase in their prices, distributed energy resources (DERs) such as wind turbines, photo voltaic systems, fuel cells and micro turbines are becoming more and more popular in electrical industry. Among the other DERs, PV systems have become more attractive because of advantages such as low maintenance requirement, noiseless operation and utilizing free source of sun. By severe growth in DERs, mostly based on renewable energy resources (RERs) with nondeterministic uncontrolled power generation, the new aspect of distribution system namely as microgrid is presented.

The microgrid can be categorized as AC-microgrids [1], DC-microgrids [2] and AC-DC-microgrids [3]. The increase in the DERs, which almost are DC power sources and the power electronic based DC loads, the aspect of DC-microgrid, is become very attractive. Connecting DERs to a common DC bus only need cheap DC/DC converters while two stages DC/DC-DC/AC is required to connect these resources to common AC bus, which increase total price, losses and volume of PEI systems. Therefore, in grids by heavy penetration of DERs, DC-microgrids is more justified in comparison with AC-microgrid.

In DER systems and DC-microgrid, power electronic interface (PEI) systems, which are responsible to connect DERs, main AC grid and DC-microgrid with different voltage ratings and types to each other, play the main role in power conversion process. Voltage source inverters (VSIs) are most popular converters in DER applications for converting DC power to AC power and inverse. However, this converter is only a buck inverter from DC side to AC. In applications, which need boost capability, an excessive step up DC/DC converter or power transformer is required which increase the PEI system costs and losses.

Moreover, VSI is vulnerable to electromagnetic interfaces (EMIs) which may lead to turning on of both upper and lower switches in inverter legs and eventually short circuiting the DC source. To cope with this problem, the Z-source inverter (ZSI) is proposed [4], which is a single stage buck-boost inverter. In this inverter, the boost capability of inverter is achieved utilizing an impedance network between DC source and inverter and dedicating shoot through cycles in ZSI pulse width modulation (PWM) algorithm. Unlike VSIs the inverter shooting through is allowable in ZSI and is a part of power conversion process.

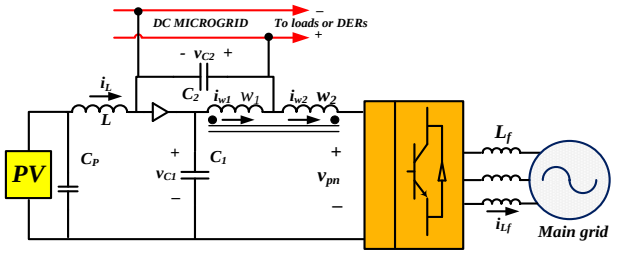

Figure 1. The proposed system configuration

The single stage power conversion in ZSI without need to any excessive step up converters, make ZSI attractive for many applications such as PV systems [5], wind turbines [6], uninterruptible power supplies [7], fuel cells [8], hybrid electric vehicles [9] etc. According to the single stage power conversion of ZSI, for proper operation of ZSI PWM, the inverter shoot through duty cycle (D) and inverter modulation index (M) is related to each other and confined each others to an upper level. Achieving boost capability with higher D leads to reduction of M, which increases voltage stress on inverter switches. Therefore, this is necessary to achieve boost capability with higher M and lower D. To this aim maximum boost and maximum constant boost control strategy based on ZSI switching algorithm is proposed to lower the voltage stress on switches [10, 11].

Addition to the control methods based on ZSI switching to reduce voltage stress on devices, in many literatures some advanced types of ZSI with higher boost capability is presented. The switched inductor ZSI has more boost capability with utilizing six excessive diodes in its impedance network [12]. Trans Z-source and T-Z-source configurations which utilizes high frequency transformers in their impedance networks rather inductors is presented in [13, 14]. Extended boost family of ZSI, which utilizes more devices in impedance network, has higher voltage gain in a lower inverter shoot through duty cycle [15].

Despite the more boost capability of high frequency transformer based ZSI structures, the increase in their boost capability requires higher turn ratio for transformer, which increase the transformer windings and volume. Asymmetrical Γ-Source inverter proposed in [16] is a high frequency transformer based ZSI which in it, unlike the other types, the boost capability of converter is increased where the transformer turn ratio is near to 1. This unique feature addressed by [16], make Γ-Source inverter a suitable choice for inverter with extended boost capability with lower volume transformer windings.

Considering the advantages of the Γ-Source inverter, this paper presents a three port converter based on Γ-Source inverter to connect PV system and DC-microgrid to the main AC grid in a single stage structure. In the proposed configuration, in a certain direction of PV panel calculated in sun tracking controller (STC), the PV system voltage is regulated using adjust of inverter shoot through duty cycle to its reference provided by maximum power point tracking (MPPT) algorithm. To avoid interaction between STC and MPPT, the STC updating intervals is considered much higher than MPPT so that in a certain direction of PV panel, MPPT sometimes can be performed.

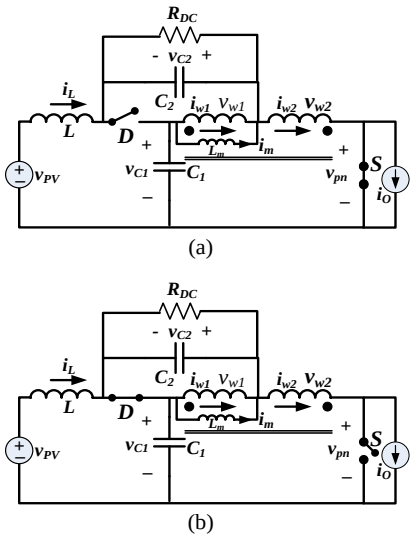

Figure 2. The equivalent circuit of the PEI system, (a) in shoot through state, (b) in nonshoot through state

For proper functioning of the sun tracking, the MPPT algorithm is stopped and PV voltage is fixed to a constant reference. This is noted that the PV bandwidth of the PV voltage controller must be high enough to fix PV voltage during sun tracking algorithm but should be lower than DC-microgrid voltage controller not to emerge as a disturbance to DC-microgrid controller. According to two degree of freedom in Γ-Source inverter control system, inverter modulation index produced in AC side current controller is dedicated to control DC-microgrid voltage. To this aim dynamic model of system is obtained for designing proper controllers for PV and DC-microgrid systems.

This paper is organized as follows. section II introduces the proposed converter system and presents the dynamic model of the system. The controller structure for regulating PV voltage and DC-microgrid voltage to its reference is proposed in section III. The dynamic model obtained in section II is used in this section for design of controllers. The performance of the proposed converter and its controller is investigated in section IV using simulation in MATLAB/Simulink environment.

II. DESCRIBTION OF THE PROPOSED SYSTEM AND MODELING

The configuration of the proposed PEI system is shown in Figure 1. In this configuration each of the available three ports are dedicated to three systems with different voltage levels and types. The input port of the Γ-Source inverter in DC side is connected to the PV system, which is only a unidirectional port. The intermediate DC link, which is a bidirectional port, is dedicated to DC-microgrid side and finally the main AC grid is connected to the PEI system through a three-phase inverter. To investigate the operation of the Γ-Source inverter as PEI system, its equivalent circuits shown in Figure 2 is used. In this figure, the injected current to main grid in view of impedance network side is modeled by a DC current source and the DC-microgrid is modeled with resistance of RDC.

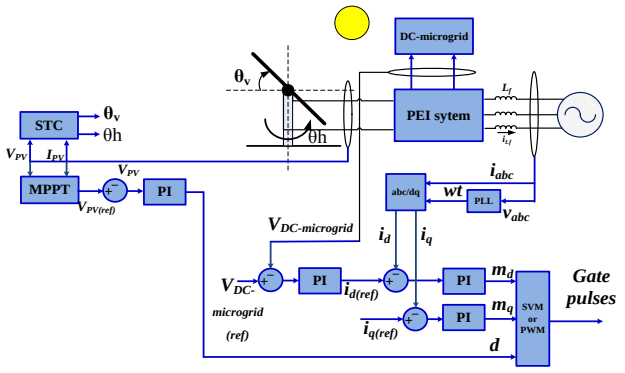

Figure 3. The proposed control system.

Moreover, the switching state of the inverter legs is modeled by a single switch of S that is turned on when the inverter is in shoot through state and is turned off when the inverter is in one of the null or active vectors in ZSI PWM algorithm. The impedance network model in shoot through condition is shown in Figure 2 (a). In this state, the switch S is turned on and diode D is reverse biased. The corresponding voltage equations in Figure 2 (a) is as:

$$v_{W1} = v_{W2} + V_{C1} \tag{1}$$

$$v_{W2} + V_{C2} + V_{PV} = v_L \tag{2}$$

$$v_{W1} = n v_{W2} \tag{3}$$

The impedance network equivalent circuit in nonshoot through state is shown in Figure 2 (b). As can be seen in this condition the switch S and diode D is respectively turned off and turned on and the current of i_o is supplied by impedance network. The voltage equations during this condition is as follows:

$$V_{C1} + v_L = V_{PV}, V_{C2} + v_{W2} + V_{PV} = v_L + v_{pn} \tag{4}$$

$$v_{W1} = -V_{C2}, V_{C1} + v_{W1} + v_{pn} \tag{5}$$

Averaging the voltages across the transformer windings and inductor to zero per switching period and neglecting parasitic resistances then results in

$$V_{C1} = \frac{1-D}{1-(2+\frac{1}{n-1})D} V_{PV} \tag{6}$$

$$V_{C2} = \frac{nD/(n-1)D}{1-(2+\frac{1}{n-1})D} V_{PV} \tag{7}$$

$$V_{pn} = \frac{1}{1-(2+\frac{1}{n-1})D} V_{PV} \tag{8}$$

where, V_{C1}, V_{C2} and V_{pn} represent the capacitor voltage across C1, C2 and inverter legs in steady state. The inverter voltage in AC side is:

$$V_{inv} = M \frac{v_{pn}}{2} \tag{9}$$

According to Equation (8), the boost capability of the asymmetrical Γ-source inverter is increased when the transformer turn ratio is near "1". This means that with a lower transformer windings and volume a high boost capability can be obtained. For dynamic modeling of the impedance network, the average state space method is used.

Considering the $x = [i_L\ i_m\ v_{C1}\ v_{C2}]^T$ as state vector of the impedance network, the state space model of the system in Figure 2 (a) is as follows:

$$\frac{dx}{dt} = A_{st}x + B_{st}u_0 \tag{10}$$

where, $u_0 = \begin{bmatrix} i_o \\ v_{PV} \end{bmatrix}$.

$$\begin{cases} A_{st} = \begin{bmatrix} -r_1/L & 0 & \frac{1}{(nL-L)} & \frac{1}{L} \\ 0 & 0 & \frac{n}{(nL_m - L_m)} & 0 \\ -\frac{1}{(nC_1 - C_1)} & \frac{-n}{(nC_1 - C_1)} & 0 & 0 \\ -1/C_2 & 0 & 0 & 0 \end{bmatrix} \\ B_{st} = \begin{bmatrix} 0 & \frac{1}{L} \\ 0 & 0 \\ 0 & 0 \\ 0 & 0 \end{bmatrix} \end{cases} \tag{11}$$

According to Figure 2 (b), in nonshoot through state the space state model of system is as follows:

$$\frac{dx}{dt} = A_{nst}x + B_{nst}u_0 \tag{12}$$

where,

$$\begin{cases} A_{nst} = \begin{bmatrix} -r_1/L & 0 & -1/L & 0 \\ 0 & 0 & 0 & -1/L \\ 1/C_1 & 0 & 0 & 0 \\ 0 & 1/C_1 & 0 & 0 \end{bmatrix} \\ B_{nst} = \begin{bmatrix} 0 & 1/L \\ 0 & 0 \\ -1/C_1 & 0 \\ (1-n)/(nC_1) & 0 \end{bmatrix} \end{cases} \tag{13}$$

Considering Equations (11) and (13), the average state model of the impedance network can be obtained as:

$$\begin{cases} \frac{dx}{dt} = Ax + Bu_0 \\ y = C_0 x \\ A = DA_{st} + (1-D)A_{nst} \\ B = DB_{st} + (1-D)B_{nst} \\ C_0 = \begin{bmatrix} 1 & 0 & 0 & 0 \\ 0 & 0 & 1 & 0 \end{bmatrix} \end{cases} \tag{14}$$

To obtain the main transfer functions of the system for design of controllers, the small signal perturbations of $\hat{D}$ and $\hat{i}_o$ are introduced which are small variations of inverter shoot through duty cycle and load current around a given operating point. Considering $\hat{D}$ and $\hat{i}_o$ as inputs, the matrix B_0, and u_0 is changed as:

$$\begin{cases} u = \begin{bmatrix} \hat{D} & \hat{i}_o \end{bmatrix}^T \\ B = \begin{bmatrix} \frac{nV_{C1}}{L(n-1)} & \frac{nV_{C1}}{L(n-1)} & \frac{-nI_L}{C_1(n-1)} & -\frac{I_m}{C_1} \\ +\frac{V_{C2}}{L} & +\frac{V_{C2}}{L} & -\frac{nI_{Lm}}{C_1(n-1)}+\frac{I_o}{C_1} & +\frac{(n-1)I_o}{nC_1} \\ \frac{-(1-D)}{C_1} & \frac{(1-n)}{nC_1} & 0 & 0 \end{bmatrix} \end{cases} \quad (15)$$

According to Equation (15), the transfer functions that should be used for controller design are as:

$$G_{\substack{\hat{V}_{C1} \\ \hat{i}_o}} = \frac{\hat{V}_{C1}}{\hat{i}_o} = [0 \quad 0 \quad 1 \quad 0](sI - A)^{-1} B \begin{bmatrix} 0 & 1 \end{bmatrix}^T \quad (16)$$

$$G_{\substack{\hat{i}_L \\ \hat{D}}} = \frac{\hat{i}_L}{\hat{D}} = [1 \quad 0 \quad 0 \quad 0](sI - A)^{-1} B \begin{bmatrix} 1 & 0 \end{bmatrix}^T \quad (17)$$

III. DESCRIBTION OF THE PROPOSED CONTROL STRATEGY

The proposed controller system is shown in Figure 3. As can be seen, the control system is composed of two control systems namely as DC-microgrid voltage controller and PV voltage controller. For design of the each part of the controller, at first the AC side current controller must be designed with a certain bandwidth as inner current controller for DC-microgrid voltage controller. Designing AC side current controller, the DC-microgrid voltage controller can be designed to regulate DC-microgrid voltage to its reference.

In this control method, the DC-microgrid voltage controller generates reference current for AC side current controller; therefore the AC current controller bandwidth must be higher than DC-microgrid voltage controller. This is noted that, since the power quality of DC microgrid is an important issue, the DC-microgrid controller must have maximum allowable bandwidth with high stability margin to properly regulate DC-microgrid voltage during its loads or sources disturbances.

Finally, the PV voltage controller must be designed with bandwidth lower than DC-microgrid voltage controller must to not emerge as a disturbance for DC-microgrid controller. Moreover, the PV voltage controller must be fast enough to be able to find maximum power point before reaching to the next implementation of the MPPT algorithm. This is noted that, the updating of maximum power point must be lower than updating period of STC to in a certain direction of PV panel; the PV system always operates in its maximum power point.

A. AC Side Current Controller

Since the AC current controller is inner controller for DC-microgrid voltage controller, it should be designed with a higher bandwidth compare to its outer voltage controller. As the grid voltage is balanced three phase, utilizing controller in synchronous reference is possible. In synchronous reference frame all variables in AC side is transformed to DC variables, therefore PI controller can be used to achieve aims such as zero steady state error and fast dynamic response. According to the AC side model of the system shown in Figure 4, the AC current controller can be designed.

Supposing the phase of grid voltage as reference phase, the direct component of current (i_d) is related to active power and quadratic component (i_q) is related to reactive power injected to grid. Considering coupling inductor with L_f = 2 mH in Figure 4, the bandwidth of current controller is set to 1 kHz where k_{Pi} = 10.5 and k_{Ii} = 16000.

Table 1. The system parameters

Circuit parameters	Values
C_1 and C_2	400 µF and 1000 µF
L	2 mH
L_m	400 µH
r_L	0.1 Ω
r_f	0.1 Ω
n	1.5
I_o	25 A
D	0.15

B. DC-Microgrid Voltage Controller

The DC-microgrid voltage controller provides current reference for direct component of AC current controller so that set the DC-microgrid voltage to its reference. Regulating the DC-microgrid voltage to a proper reference value make balance between the PV power generating and injected power to main grid and DC-microgrid. For example, when the PV power increases, its excessive energy that is not transferred to grid is stored in C_2, which increase its voltage higher than its reference. In this condition, the AC current controller must increase the active power injected to grid to subside capacitor voltage to its reference.

Inversely, when PV power drops, the injected power to grid is become higher than PV power, which leads to decrease of capacitor voltage. When the capacitor voltage controller senses the drop in capacitor, it reduces the active power to grid to increase capacitor voltage to its reference voltage. Achieving above mentioned requirements, the coefficients of capacitor controller must be negative. In other view, when the DC-microgrid load demand is increased/decreased, the DC-microgrid voltage is reduced/increased, therefore in a certain power generating of PV, the active component of AC current must be reduced/increased to keep the DC-voltage to its reference.

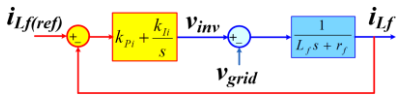

Figure 4. AC current controller model in Laplace domain

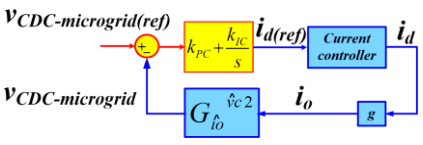

Figure 5. Controller model of capacitor voltage in Laplace domain

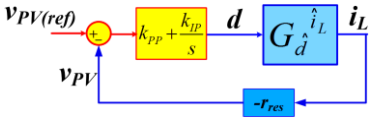

Figure 6. PV voltage controller model in Laplace domain

During this transients, the PV voltage controller must set PV voltage to its reference but if its bandwidth not being lower than DC-microgrid controller, the dynamic o PV voltage controller emerges as another source of disturbance and prolong transients or even may make system unstable. In AC current controller the i_q is set to zero to eliminate reactive power exchange with grid. The capacitor voltage controller model in Laplace domain is shown in Figure 5. In this figure, i_o is related to i_d with coefficient of (g) which is a constant value in a certain modulation index and inverter shoot through duty cycle. According to the impedance network specification listed in Table 1, the bandwidth of DC-microgrid voltage controller is set to 100 Hz with K_{PC} = -0.1 and K_{IC} = -20.

C. PV Voltage Controller

Setting DC-microgrid voltage to its reference, the PV voltage controller can be designed with a specific bandwidth lower than DC-microgrid voltage controller and fast enough to find maximum power point in a desirable time. The inverter shoot through duty cycle is due to regulate the PV voltage to its reference provided by MPPT in a certain direction of PV panel. The PV voltage controller model in Laplace domain is shown in Figure 6. In this figure, (r_{res}) significant the equivalent resistance of PV module around its operating point. Considering the capacitor voltage regulated to its reference, increase in D lead to lowering the PV voltage and inversely PV voltage is increased when D is reduced, therefore the PV voltage controller parameters must be negative.

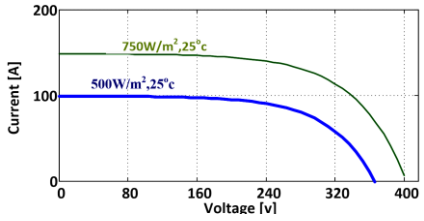

(a)

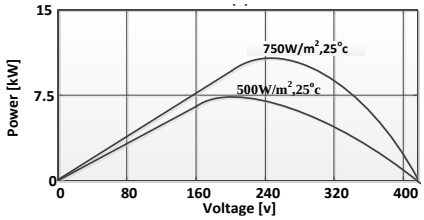

(b)

Figure 7. PV characteristic curves, (a) Voltage-Current, (b) Voltage- Power

According to system parameters and supposing r_{res} = 4, the PV voltage controller is designed with bandwidth of 25 Hz where K_{PP} = -0.002 and K_{IP} = -0.1. As can be seen, the bandwidth of the PV voltage controller is lower than DC-microgrid voltage controller, which discourage dynamic interactions between PV voltage, and capacitor voltage controller. The settling time of the PV voltage controller is about 30 ms which is suitable for updating period of some seconds for MPTT algorithm. To allow the MPPT algorithm is completed some times before updating the PV panel direction, the updating period for STC is considered some minutes.

D. Sun-Tracker Controller

The PV voltage-current and voltage-power characteristic curve is shown in Figure 7. As can be seen in a certain PV voltage, the generated power by PV is dependent to the sun intensity and PV panel surface temperature. As mentioned, the updating period of MPPT algorithm is lower than STC. However, for obtaining a proper direction for PV panel, during the implementation of sun tracking algorithm, the PV voltage is kept to a constant reference and MPPT algorithm is ceased. Keeping the PV voltage to a constant voltage while the PV panel direction is varying, changes the sun intensity on PV panel such that when the panel direction is near to direction of sun, the sun intensity increases and inverse.

For tracking of the sun, the PV panel horizontal and vertical angle must be changed in some steps. To this aim for example at first time, the vertical angle varies in some steps to find maximum power point and then horizontal angle varies to find the maximum power point in a certain vertical angle. Since the PV voltage controller is designed with the bandwidth of 25 Hz, which its time constant is much higher than STC, the implementation of the sun-tracking algorithm does not affect the PV voltage. By ending the sun-tracking algorithm, the MPPT algorithm again is performed to find the maximum power point.

IV. SIMULATION RESULTS

To evaluate the efficiency of the proposed control method, a typical PV DC-microgrid system is considered. The system is modeled in MATLAB/Simulink and its operation is considered during the load change in DC-microgrid side, during the implementation of MPPT algorithm and finally during the process which in it the sun tracking is functioning to find the sun direction.

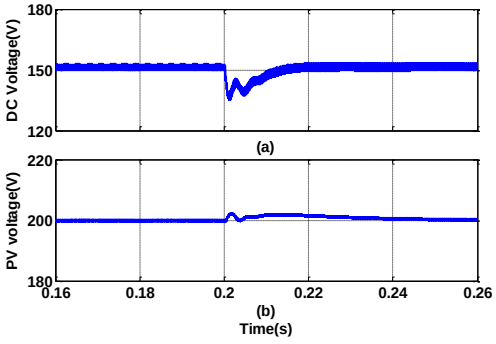

Figure 8. Load changes in DC-microgrid, (a) DC-microgrid voltage, (b) PV voltage

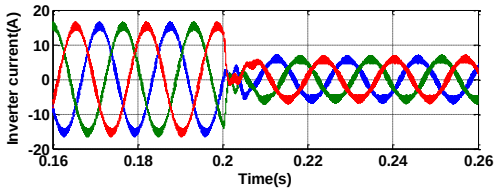

Figure 9. Inverter current

The system parameters and controller coefficients are the same, which is mentioned later within the text. As mentioned, it is required that the DC-microgrid bandwidth be higher than PV voltage controller while the PV voltage be faster than the sun tracker controller. To this aim, according to the controllers designed in section III, the DC-microgrid bandwidth is 100 Hz while PV voltage controller is designed with bandwidth of 25 Hz. The considered bandwidth for PV control system is lower than DC-microgrid, therefore the PV side disturbances have minor effect on DC-microgrid.

Moreover, bandwidth of the PV controller has high enough to track PV voltage reference during implementation of MPPT algorithm. This is noted that, the designed bandwidth for PV controller is high enough to fix PV voltage to its reference while STC change the PV panel direction to find the sun. The operation of the control system during the load change in DC-microgrid is shown in Figure 8. At first, total load in DC-microgrid is 3.5 kW. At t = 0.2 s, a step load change occurs in DC-microgrid and total load reaches to 7 kW. The DC-microgrid voltage during the load change is shown in Figure 8 (a).

In the instance of the load change, the DC-microgrid drops about 10 V and after 10ms, voltage backs to its reference value. The PV voltage during load change in DC-microgrid is shown in Figure 8 (b). As can be seen the PV voltage is set to its reference value of 200 V with a little deviation (about 2 V) during the transients caused by load change in DC-microgrid side.

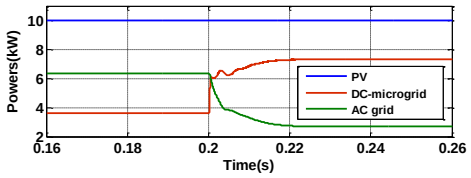

Figure 10. DC-microgrid PV system power exchanges

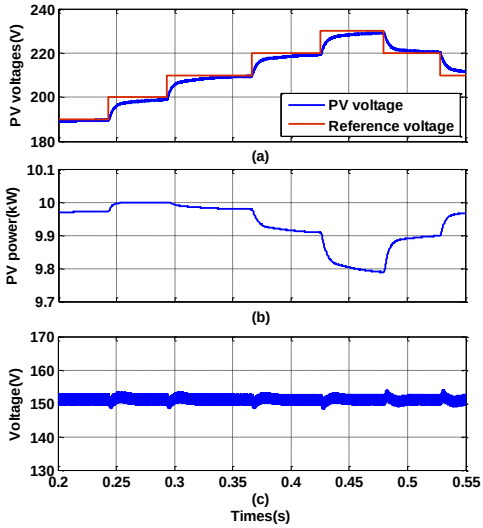

Figure 11. MPPT algorithm, (a) PV voltage, (b) PV power, (c) DC-microgrid voltage

As known, the DC-microgrid is regulated using adjust of the inverter current injected to grid. The Inverter current injected to grid is shown in Figure 9. As can be seen, the load change in DC-microgrid leads the inverter current phase to be inversed. Inversion in inverter current means the change in power flow direction between inverter and main grid.

The power components of the DC-microgrid PV system is shown in Figure 10. Considering a constant weather condition and fixing the PV voltage to 200 V, the PV power is always 10 kW. Increasing in the load from 3.5 kW to 7 kW in DC-microgrid is shown in Figure 10. Since the PV power is fixed to its reference and the DC-microgrid is increased, the absorbed power from grid must be increased to supply load power in DC-microgrid.

The grid power is shown in Figure 10. As can be seen before the load change the power is injected from inverter to grid while after increasing the load, power is absorbed from the main grid. To evaluate performance of the control system during implementation of the maximum power point tracking algorithm, the PV voltage reference is changed in some steps in the way shown in Figure 11 (a). As can be seen the PV voltage track its reference properly with settling time of about 40ms. The PV generated power is shown in Figure 11 (b). As can be seen, the PV power is changed when the PV voltage is varied.

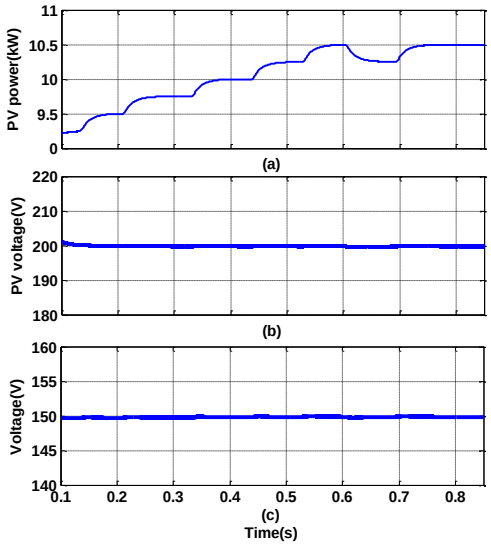

Figure 13. Sun tracking algorithm, (a) PV power, (b) PV voltage, (c) DC-microgrid voltage

Considering the variation of the PV power, the MPPT algorithm can determine the maximum power point during implementation of MPPT algorithm. The DC-microgrid voltage is shown in Figure 11 (c) which is set to its reference of 150 V during the voltage variations in PV voltage. As mentioned, the sun tracking algorithm updating is in range of minutes. The proper operation of the sun-tracking algorithm requires the proper operation of the PV voltage controller to set the PV voltage to its reference voltage. This is noted that during the functioning sun tracking algorithm, the MPPT algorithm is stopped temporarily to set the PV voltage to a specific reference voltage. The operation of the sun-tracking algorithm is shown in Figure 12.

The variations in PV panel direction leads to change in PV power production. This is noted that the duration of variations in the PV panel direction is about some seconds that here is exaggerated to some tens of (ms). Moreover, this is supposed that the PV angle is only varied in one of the horizontal or vertical directions. The variation in PV panel angle leads to variation of sun light power per area. According to Figure 7, the variation in sun light power per area in a constant PV voltage leads to variation in PV power, therefore determining the maximum power means finding the sun direction.

The PV power during the variation of PV panel angle is shown in Figure 13 (a). As can be seen, the angle, which in it the PV power reaches, to 10.5 kW is the right angle with direction toward the sun. Regulating the PV voltage to a constant voltage is an important condition for proper functioning of the sun-tracking algorithm. The PV voltage is shown in Figure 13 (b) which always is fixed to its reference of 200 V. The DC-microgrid voltage during the implementation of sun tracking algorithm is shown in Figure 13 (c). As can be seen its voltage is regulated to 150 V, which is reference voltage.

V. CONCLUSIONS

This pas paper has proposed a power electronic converter for connecting three different voltages of main AC grid, DC-microgrid and PV system to each other with minor power converter requirements. To this aim, a controller is designed to regulate PV voltage on its reference voltage while fixing the DC-microgrid voltage to its rated voltage. To eliminate disturbance effect of the PV voltage controller on DC-microgrid voltage, the bandwidth of the PV voltage controller is considered lower than the DC-microgrid voltage controller.

Moreover, the PV voltage controller is designed fast enough for proper operation of the sun tracking algorithm and lowering its interference with MPPT controller. Therefore, during the variations in PV panel direction, the PV voltage is fixed to its reference, which is required to find proper direction of sun. The performance of the PV voltage controller, the DC-microgrid voltage controller is confirmed using simulation results in MATLAB/Simulink.

REFERENCES

[1] K. Sao, P.W. Lehn, "Control and Power Management of Converter Fed MicroGrids", IEEE Trans. Power Syst., Vol. 23, No. 3, pp. 1088-1098, Aug. 2008.

[2] A. Sannino, G. Postiglione, M.H.J. Bollen, "Feasibility of a DC Network for Commercial Facilities", IEEE Trans. Ind. Appl., Vol. 39, No. 5, pp. 1409-1507, Sep. 2003.

[3] X. Liu, P. Wang, P.C. Loh, "A Hybrid AC/DC Microgrid and its Coordination Control", IEEE Trans. Smart Grid, Vol. 2, No. 2, pp. 278-286, Jun. 2011.

[4] F.Z. Peng, "Z-Source Inverter", IEEE Trans. Ind. Applicat., Vol. 39, pp. 504-510, Mar. /Apr. 2003.

[5] D. Cao, S. Jiang, X. Yu, F.Z. Peng, "Low-Cost Semi-Z-Source Inverter for Single-Phase Photovoltaic Systems", IEEE Trans. Power Electron., Vol. 26, No. 12, pp. 3514-3523, Dec. 2011.

[6] S. Zhang, K. Tseng, et al., "Design of a Robust Grid Interface System for PMSG-Based Wind Turbine Generators", IEEE Trans. Ind. Electron., Vol. 58, No. 1, pp. 316-328, Jan. 2011.

[7] Z.J. Zhou, X. Zhang, P. Xu, W.X. Shen, "Single-Phase Uninterruptible Power Supply Based on Z-Source Inverter", IEEE Trans. Ind. Electron., Vol. 55, No. 8, pp. 2997-3003, Aug. 2008.

[8] J. Jung, A. Keyhani, "Control of a Fuel Cell Based Z-Source Converter", IEEE Trans. Ind. Electron., Vol. 22, No. 2, pp. 467-476, Jun. 2007.

[9] F.Z. Peng, M.S. Shen, K. Holland, "Application of Z-Source Inverter for Traction Drive of Fuel Cell-Battery Hybrid Electric Vehicles", IEEE Trans. Power Electron., Vol. 22, No. 3, pp. 1054-1061, May 2007.

[10] F.Z. Peng, M. Shen, Z. Qian, "Maximum Boost Control of the Z-Source Inverter", IEEE Trans. Power Electron., Vol. 20, No. 4, pp. 833-838, Jul./Aug. 2005.

[11] M. Shen, J. Wang, A. Joseph, F.Z. Peng, "Constant Boost Control of the Z-Source Inverter to Minimize Current Ripple and Voltage Stress", IEEE Trans. Ind. Applicant, Vol. 42, No. 3, pp. 770-778, May/June 2006.

[12] M. Zhu, K. Yu, F.L. Luo, "Switched Inductor Z-Source Inverter", IEEE Trans. Power Electron., Vol. 25, No. 8, pp. 2150-2158, Aug. 2010.

[13] W. Qian, F.Z. Peng, H. Cha, "Trans-Z-Source Inverters", IEEE Trans. Power Electron., Vol. 26, No. 12, pp. 3453-3463, Dec, 2011.

[14] M.K. Nguyen, Y.C. Lim, Y.G. Kim "TZ-Source Inverters", IEEE Trans. Ind. Electron., Vol. 60, No. 12, pp. 5686-5695, Dec. 2013.

[15] C.J. Gajanayake, L.F. Lin, et al., "Extended Boost Z-Source Inverters", IEEE Trans. Power Electron., Vol. 25, No. 10, pp. 2642-2652, Oct. 2010.

[16] W. Mo, P.C. Loh, F. Blaabjerg, "Asymmetrical Γ-Source Inverters", IEEE Trans. Ind. Electron., Vol. 61, No. 2, pp. 637–647, Feb. 2014.

[17] Hosseini, M. Farsadi, A. Lak, H. Ghahramani, N. Razmjooy, "A Novel Method Using Imperialist Competitive Algorithm (ICA) for Controlling Pitch Angle in Hybrid Wind and PV Array Energy Production System", International Journal on Technical and Physical Problems of Engineering (IJTPE), Issue 11, Vol. 4, No. 2, pp. 145-152, June 2012.

[18] S. Nema, R.K. Nema, G. Agnihotri, "MATLAB/Simulink Based Study of Photovoltaic Cells/Modules/Array and their Experimental Verification", International Journal of Energy and Environment, Vol. 1, Issue 3, pp. 487-500, 2010.

BIOGRAPHIES

Farzad Khoshkhati received the B.Sc. degree in Electrical Engineering from University of Zanjan, Zanjan, Iran (2006-2011) and M.Sc. degree in Mechatronics from University of Tehran, Tehran, Iran (2011-2013).

Siroos Toofan received the B.Sc. degree in Electronics Engineering from Amirkabir University of Technology (Tehran Polytechnic), Tehran, Iran in 1999, and the M.Sc. and Ph.D. degrees in Electronics Engineering form the Iran University of Science and Technology (IUST), Tehran, Iran in 2002 and 2008, respectively. From 2007 to 2008, on his sabbatical leave, he was with the VLSI group of Politechnico di Torino and in the Microelectronics Integrated Circuits Lab. of the Politechnico di Milano Universities in Italy. He has been working as Assistant Professor with the Department of Electrical Engineering, University of Zanjan, Zanjan, Iran since 2009. His current research activities include the design of CMOS analog integrated circuits, RF integrated circuits, capacitive sensors readout circuits and energy harvesting circuits.

Behzad Asaei received the B.Sc. and M.Sc. degrees from the University of Tehran, Tehran, Iran, in 1988 and 1990, respectively, and the Ph.D. degree from the Sydney University, NSW, Australia, in 1995, all in Electrical Engineering. Since 2006, he has been the Director of the Energy and Automotive Technology Laboratory, School of Electrical and Computer Engineering, University of Tehran, Tehran, Iran. His research interests include the field of automotive electronics, solar energy, electric and hybrid electric vehicles, power electronics, and motor drives in which several projects including two electric vehicles, hybrid electric locomotive, solar car, hybrid motorcycle, electric bike, and automotive electronics are completed.